Limits on Anomalous Spin-Spin Couplings between Neutrons

Alexander G. Glenday,[1,2] Claire E. Cramer,[1] David F. Phillips,[1] and Ronald L. Walsworth[1,2]

[1]*Harvard-Smithsonian Center for Astrophysics, Cambridge, Massachusetts 02138, USA*

[2]*Department of Physics, Harvard University, Cambridge, Massachusetts 02138, USA*

(Received 9 April 2008; published 23 December 2008)

We report experimental limits on new spin-dependent macroscopic forces between neutrons. We measured the nuclear Zeeman frequencies of a ^{3}He/^{129}Xe maser while modulating the nuclear spin polarization of a nearby ^{3}He ensemble in a separate glass cell. We place limits on the coupling strength of neutron spin-spin interactions mediated by light pseudoscalar particles like the axion $[g_p g_p/(4\pi\hbar c)]$ at the 3×10^{-7} level for interaction ranges longer than about 40 cm. This limit is about 10^{-5} the size of the magnetic dipole-dipole interaction between neutrons.

DOI: 10.1103/PhysRevLett.101.261801 PACS numbers: 13.40.Gp, 11.30.Cp, 14.80.Mz, 32.60.+i

Searches for new spin-dependent macroscopic forces explore possible physics beyond the standard model, such as Lorentz symmetry violation and the existence of new particles like the axion. Searches for anomalous couplings between spins have typically been interpreted in terms of forces mediated by the axion, which is of interest as a solution to the strong *CP* problem and a dark matter candidate [1]. In more recent theoretical work, Arkani-Hamed and co-workers have considered the dynamical effects of broken Lorentz symmetry added to the standard model, which include new spin-dependent forces [2]. A phenomenological theory developed by Dobrescu and Mocioiu enumerates all possible spin-dependent forces that satisfy rotational invariance and standard assumptions of quantum field theory [3]. This theory includes axion-mediated forces as well as the more complex Lorentz symmetry violation considered by Arkani-Hamed and co-workers. In all cases, the strength of the coupling between spins is dependent on the particle species, e.g., electron, neutron, proton, and so a complete experimental survey should cover all particle combinations. There are existing experimental limits on coupling of electron spins to all other species [4–6], as well as a limit on proton-proton coupling [7], but there is no published limit on neutron-neutron spin coupling.

To measure new couplings between neutron spins we monitored the nuclear Zeeman frequencies of a ^{3}He/^{129}Xe maser, our detector for new spin-dependent forces, while modulating the nuclear spin polarization of an ensemble of ^{3}He atoms in a separate cell, our spin source. Anomalous dipole-dipole couplings between the longitudinally polarized source and maser spins will lead to an additional torque on the precessing maser spins and thus a frequency shift. The two-species ^{3}He/^{129}Xe maser has been described previously [8–12]; here we provide a brief review of its design and operation (see schematic in Fig. 1). Colocated ensembles of ^{129}Xe and ^{3}He atoms at pressures of hundreds of Torr are held in a double-chamber glass cell placed in a homogeneous magnetic field of 6 G. Both species have spin-1/2 nuclei and the same sign nuclear magnetic dipole moment, but no higher-order electric or magnetic nuclear multipole moments. In one chamber of the glass cell, the pump bulb (maintained $\approx$135 °C), the noble gas atoms are pumped into a nuclear Zeeman population inversion by contact interactions with optically pumped Rb vapor [13]. The noble gas atoms diffuse into the second chamber, the maser bulb (maintained $\approx$45 °C), which is surrounded by an inductive coil connected to a circuit resonant at both the ^{3}He and ^{129}Xe nuclear Zeeman frequencies (19.6 and 7.1 kHz, respectively). For a sufficiently high flux of population-inverted nuclear magnetization, active maser oscillation of both species can be maintained indefinitely. The maser is protected from external magnetic fields by three layers of magnetic shielding. By comparing one of the noble-gas masers to a stable frequency reference (a hydrogen maser), we can stabilize the magnetic field and then use the other noble-gas maser as a sensor for new spin-dependent forces. This application relies on the fact that the gyromagnetic ratios of ^{3}He and ^{129}Xe differ by a factor of $\sim$2.75, whereas the coupling to new spin-dependent forces should be very similar for the two noble gas species since the neutron is the primary

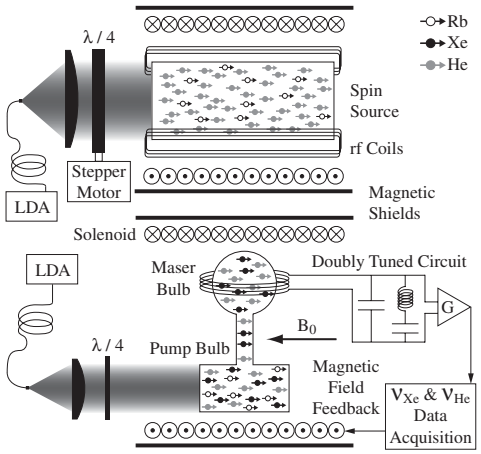

FIG. 1. Experimental schematic showing the ^{3}He spin source on top and the ^{3}He/^{129}Xe maser on the bottom (not to scale).

contributor to the nuclear spin for both ^{3}He and ^{129}Xe (approximately 87% [14] and 75% [15], respectively, and with uncertainties that do not affect results reported here). For all the measurements reported in this Letter the magnetic field was locked using the ^{129}Xe maser frequency referenced to a hydrogen maser. Thus the difference between the ^{3}He maser frequency and the reference is given by

$$\nu_{\mathrm{He}} - \frac{\gamma_{\mathrm{He}}}{\gamma_{\mathrm{Xe}}}\nu_{\mathrm{Xe}} \approx \left(0.87 - 0.75\frac{\gamma_{\mathrm{He}}}{\gamma_{\mathrm{Xe}}}\right)\nu_{\mathrm{SF}} \approx -1.2\nu_{\mathrm{SF}},$$

where ν_{He} and ν_{Xe} are the respective ^{3}He/^{129}Xe maser frequencies, γ_{He} and γ_{Xe} are the respective ^{3}He/^{129}Xe gyromagnetic ratios, and ν_{SF} is the frequency shift due to an anomalous spin-dependent force between neutrons.

Recent upgrades to the ^{3}He/^{129}Xe maser have yielded an order of magnitude improvement in frequency stability on time scales of hours, relative to earlier versions of the device [10–12]. These upgrades include optimization of the noble gas pressures, double bulb cell geometry, and the temperature control and optical pumping systems to maximize maser amplitudes and coherence times, as well as an increase in main magnetic field and hence Zeeman frequency to increase maser power.

For the neutron spin source we used a valved Pyrex glass cell filled with 6.5 amagat of ^{3}He, 0.2 amagat of N_2, and 100 mg of Rb (see schematic in Fig. 1). The cell is a cylinder with total volume of 88 cm^3 (12 cm long, 3 cm diameter) and is housed inside an insulated glass oven heated to 160 °C with blown air. The oven is surrounded by a pair of rf coils designed to efficiently invert the ^{3}He spin polariztion via adiabatic fast passage. The rf coil field homogeneity (few percent across the cell) ensures accurate determination of the ^{3}He polarization by measuring the amplitude of spin precession induced by resonant NMR pulses. The cell is centered inside a solenoid, which provides a static magnetic field of 1 G and serves as the spins' quantization axis (parallel to the maser's magnetic field). The solenoid has separate end coils to optimize the magnetic field homogeneity, which is achieved by maximizing the ^{3}He spin coherence time in the spin source. The high homogeneity of the static magnetic field is necessary to minimize polarization loss due to diffusion through transverse field gradients. Also, the relatively long ^{3}He spin coherence time ($\sim$2 sec) improves polarization measurement accuracy by avoiding dead-time errors between inducing and measuring the spin precession. A cylindrical magnetic shield (38 cm diameter) with end caps surrounds the spin source. A laser diode array (LDA) shines 25 W of Rb D1 resonant ($\sim$795 nm), circularly polarized light onto the cell, spin polarizing the ^{3}He to $12 \pm 1\%$ by spin-exchange collisions with the optically pumped Rb. Given this level of polarization the spin source contains 1.8×10^{21} polarized ^{3}He spins located 41 cm from the maser bulb of the ^{3}He/^{129}Xe maser (determined relative to the center of the spin source cell and maser bulb).

To modulate the orientation of the ^{3}He spins in the source, we adiabatically transferred the spins between states by sending a drive signal through the rf coils and scanning this rf signal through the Zeeman resonance on a time scale of $\sim$100 m sec. The adiabatic transfer was very efficient with only 0.1% fractional loss of total polarization per transfer, as measured by the change in amplitude of induced ^{3}He spin precession after multiple transfers. In order to maintain a high ^{3}He polarization level, the angular momentum delivered by the laser must always be in the same direction as the ^{3}He spins, so we inverted the quarter wave plates using a stepping motor each time we adiabatically reversed the ^{3}He spin state (Fig. 1). The spins and quarter wave plates were typically reversed once every 20 min to maximize the ^{3}He/^{129}Xe maser sensitivity given white phase noise at short times and long term drifts (see Fig. 2) and to avoid room temperature and other system parameter oscillations which have shorter periods.

We collected ^{3}He maser frequency data for approximately 85 days, resulting in a data set of 3054 modulation periods of the spin source. We analyzed the data in blocks of one spin source modulation period using a least-squares fit of the phase of the ^{3}He maser to the time integrated state of the ensemble ^{3}He spin in the source (a triangle wave). To eliminate the effects of linear frequency drift, fits were calculated starting every half period giving a total of 6107 fits. We performed fits on the time variation of maser phase (rather than frequency) to retain a χ^2 distribution of the sum of squares of residuals since the (approximately square wave) spin modulation has significant harmonic components in the white phase noise spectrum of the data (Fig. 2). Phase noise was estimated using the modified Allan deviation of the ^{3}He maser frequency. We rejected fits whose sum of squares of residuals had less than 5% probability given the χ^2 distribution (final results are insensitive to the choice of cutoff), leaving a data set of 4966 fits. Figure 3 shows the distribution of these fit amplitudes converted from phase to frequency. The weighted mean of fit amplitudes that passed the χ^2 test gives a shift of the ^{3}He Zeeman frequency of 1.9 ± 6.1 nHz (1σ uncertainty). The standard error of this weighted mean was determined using the number of independent modulation periods included in determining the mean (2483). We verified our fitting procedure using a Monte Carlo simulation of the data.

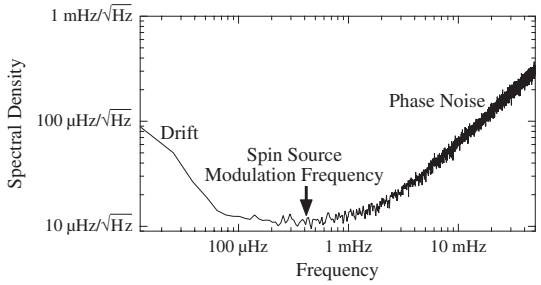

FIG. 2. Noise spectrum of the ^{3}He Zeeman maser frequency averaged from three weeks of data. The modulation period of the spin orientation of the spin source was chosen to lie in the white frequency noise dominated part of the spectrum to avoid phase noise at high frequencies and drift at low frequencies.

The leading systematic error was the limitation of the magnetic shields and maser comagnetometry to reject magnetic coupling to the spin source. To test this limitation we performed separate experiments in which we modulated the 1 G quantizing magnetic field of the spin source with the same period that we modulated the spins in the spin source. At the location of the maser bulb this applied magnetic field is 5.5×10^4 larger than the field from the magnetization of the ^{3}He spins in the spin source. We set a limit of 50 nHz on variation of the ^{3}He maser frequency induced by the modulated magnetic field, which, after rescaling to the field generated by the spin source, means that this systematic effect is <1 pHz, far below our statistical sensitivity to anomalous spin-spin couplings.

To interpret the significance for theoretical models of the experiment presented here, we simplify the theoretically proposed new spin-spin interactions to only include parallel spin cases. For example, the potential between two parallel neutron spins mediated by the axion and axionlike pseudoscalar particles is (in SI units)

$$V(r) = \frac{g_p^n g_p^n}{4\pi\hbar c}\frac{\hbar^3}{4m_n^2 c}\left(\frac{1}{\lambda r^2} + \frac{1}{r^3}\right)e^{-r/\lambda}, \qquad (1)$$

where $g_p^n g_p^n/(4\pi\hbar c)$ is the dimensionless coupling constant, m_n is the neutron mass, r is the separation between spins, and λ is the Compton wavelength of the axionlike particle that determines the range of the interaction [1]. While constraints on the axion interaction from astrophysical observations correspond to $\lambda \sim 20$ cm to 200 μm [16], other axionlike pseudoscalars are not constrained in this way [17]. Our measurement, when interpreted in terms of an axionlike mediated force between neutrons and including finite-sample-size effects, leads to a 1σ limit of $g_p^n g_p^n/(4\pi\hbar c) < 3 \times 10^{-7}$ for distances longer than about 41 cm, with the full exclusion region shown in Fig. 4. The theoretical estimate for the size of $g_p^n g_p^n/(4\pi\hbar c)$ for axions that would solve the strong CP problem is 5×10^{-30} m$^2/\lambda^2$, which is far below our limit or any that could be set with a similar experiment [18].

Next we consider the broken symmetry proposed by Arkani-Hamed and co-workers, which gives rise to Goldstone bosons whose exchange between fermions leads to a long-range $1/r$ spin-dependent potential [2]. The potential also depends on where the spins being measured are located relative to the spin source that generates the potential and its motion relative to the background field of Goldstone bosons. The form of the Goldstone boson mediated potential between two parallel spins is (in SI units, except where noted)

$$V(r) = -\left(\frac{M}{F}\right)^2 \frac{\hbar c}{8\pi}\frac{1}{r}A(\alpha, \gamma, \theta_v), \qquad \alpha = M\frac{rv}{\hbar c^2},$$
$$\gamma = M\frac{Rv}{\hbar c^2}, \qquad \cos\theta_v = \hat{r}\cdot\hat{v}, \qquad (2)$$

where M (given in eV) is the spontaneous symmetry breaking scale, F (given in eV) is the mass scale determining the strength of the coupling to Dirac fermions ($\frac{M}{F}$ is the dimensionless coupling), r is the separation between spins, and R is the radius of the spin source. The final term, $A(\alpha, \gamma, \theta_v)$, gives a parabolic shadow in the wake and shock waves in front of the spin source as it moves at velocity v with respect to the rest frame of the background field (see Fig. 5), which is taken to be the rest frame of the cosmic microwave background (CMB). The velocity of the spin source relative to the CMB rest frame is assumed to be given by the dipole moment of the CMB, which has been measured as $1.23 \times 10^{-3}c$ [19]. This gives a vector that sweeps out a cone (inner angle of 166°) in the local lab frame over the course of a sidereal day. As a further simplification to the potential we only consider interactions in the parabolic shadow region of $A(\alpha, \gamma, \theta_v)$, whose boundary with the shock wave region is well approximated by $x = 3.15 - 0.0796y^2$, where $y = \alpha\sin\theta_v$ and $x = \alpha\cos\theta_v$, for $\gamma < 1$. For larger γ the parabola is still an excellent approximation for $\alpha > 5\gamma$ where errors only develop in the offset of the parabola (~20% for $\gamma = 10$). The value of $A(\alpha, \gamma, \theta_v)$ in the shadow region is approximated as being uniformly 0.7 (the average value of A for most transits across the shadow region) and the shock wave region is set to zero. Errors introduced by these approximations and finite-sample-size effects were all on the same scale, or smaller, than experimental uncertainties.

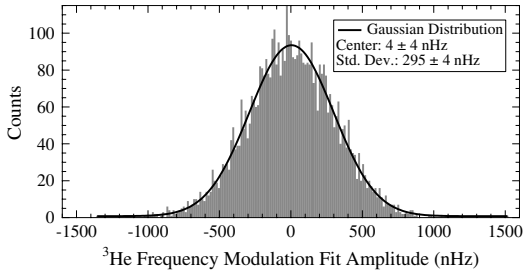

FIG. 3 (color online). Distribution of frequency modulation amplitudes from the fit of the ^{3}He Zeeman maser frequency to the modulated spin orientation of the spin source. The amplitudes have a Gaussian distribution that agrees well with the noise spectrum shown in Fig. 2.

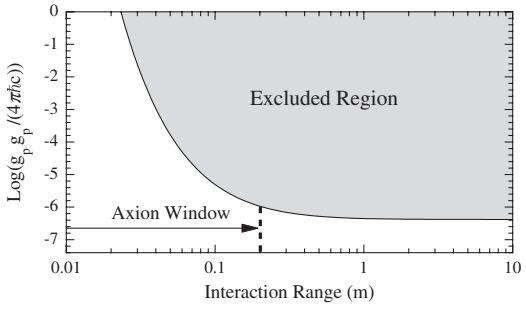

FIG. 4. 1σ excluded region from the present experiment for the dimensionless coupling constant $g_p^n g_p^n/(4\pi\hbar c)$ as a function of interaction range for a neutron-neutron spin interaction mediated by the axion or an axionlike pseudoscalar particle [see Eq. (1)].

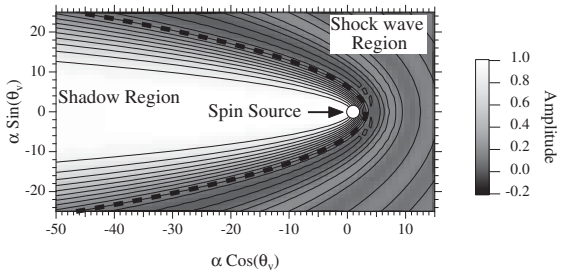

FIG. 5. Calculation of amplitude $A(\alpha, \gamma, \theta_v)$ for $\gamma = 0$ for the Goldstone boson mediated potential between two parallel spins [see Eq. (2)]. The dashed line is the parabolic approximation for the boundary between the shadow and shock wave regions.

The sensitivity of our experiment to the potential derived by Arkani-Hamed and co-workers [Eq. (2)] depends on M, as this determines the width of the parabolic wake generated by the spin source and hence the fraction of the sidereal day for which there is any potential to measure. For example, for values of $M < 1$ meV, at which point there is a nonzero potential between the spins for the whole day, we find a 1σ limit of $\frac{M}{F} < 4 \times 10^{-19}$. The exclusion region due to the spin-spin potential is shown in the center of Fig. 6, where the fractional averages of the full data set used to calculate each point are all consistent with zero. The left-hand side of the figure shows the regime where the effective field theory breaks down and is no longer predictive. The right-hand side of the figure includes the bounds previously set by the ^{3}He/^{129}Xe maser for a Lorentz violating background field as the Earth, and hence the experiment, rotated over a sidereal day [2,11]. While there is no theoretical estimate for the size of M or F, the Goldstone bosons that mediate the spin force have particular cosmological significance for two values of M. If $M \sim 1$ meV then the bosons could be dark energy, and if $M \sim 1$ eV then the bosons could be a dark matter candidate.

Finally, we consider the phenomenological theory developed by Dobrescu and Mocioiu, which contains nine new spin-dependent potentials. Six of these depend on the relative velocity between the spins (zero in our experiment). Of the remaining three potentials, one is the same as the axion potential and one requires perpendicular rather than the parallel spin orientation in our experiment. This

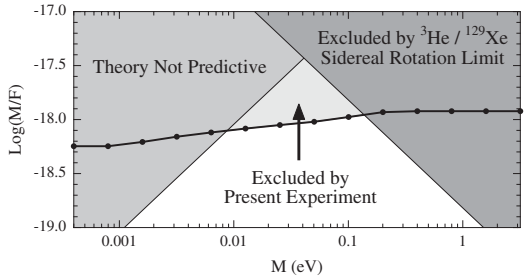

FIG. 6. 1σ excluded region from the present experiment for neutron-neutron spin coupling as described by Eq. (2) (see text).

leaves the following potential between two parallel spins (in SI units)

$$V(r) = -\frac{g_A^n g_A^n}{\hbar c}\frac{\hbar c}{4\pi}\frac{1}{r}e^{-r/\lambda}, \quad (3)$$

where $g_A^n g_A^n/(\hbar c)$ is the dimensionless coupling constant, r is the separation between spins, and λ is the interaction range [3]. From our experimental data we find a 1σ bound on this potential of $g_A^n g_A^n/(\hbar c) < 2 \times 10^{-37}$ for distances greater than about 41 cm. There is no theoretical expectation for the size of this coupling, but we note that a limit on analogous electron-electron interactions $g_A^e g_A^e/(\hbar c) < 4 \times 10^{-35}$ has been set [3].

In conclusion, we have used a ^{3}He/^{129}Xe maser and a separate ensemble of spin-polarized ^{3}He to perform an experimental search for new spin-dependent forces between neutrons. This experiment sets bounds on several theoretical frameworks for physics beyond the standard model that include Lorentz symmetry violation and particles that are candidates for dark matter. Further improvement in these results could come from higher density spin sources and improved comagnetometers [20].

We acknowledge useful discussions with Jesse Thaler and Michael Crescimanno. This work was supported by NSF grant PHY-0502279.

[1] J. E. Moody and F. Wilczek, Phys. Rev. D **30**, 130 (1984).
[2] N. Arkani-Hamed *et al.*, J. High Energy Phys. 7 (2005) 029.
[3] B. A. Dobrescu and I. Mocioiu, J. High Energy Phys. 11 (2006) 005.
[4] D. J. Wineland *et al.*, Phys. Rev. Lett. **67**, 1735 (1991).
[5] T. C. P. Chui and W. T. Ni, Phys. Rev. Lett. **71**, 3247 (1993).
[6] W. T. Ni *et al.*, Physica (Amsterdam) **194B**, 153 (1994).
[7] N. F. Ramsey, Physica (Amsterdam) **96A**, 285 (1979).
[8] T. E. Chupp *et al.*, Phys. Rev. Lett. **72**, 2363 (1994).
[9] R. E. Stoner *et al.*, Phys. Rev. Lett. **77**, 3971 (1996).
[10] D. Bear *et al.*, Phys. Rev. A **57**, 5006 (1998).
[11] D. Bear *et al.*, Phys. Rev. Lett. **85**, 5038 (2000).
[12] F. Cane *et al.*, Phys. Rev. Lett. **93**, 230801 (2004).
[13] T. G. Walker and W. Happer, Rev. Mod. Phys. **69**, 629 (1997).
[14] The contribution of the neutron to the ^{3}He spin is determined from deep inelastic scattering of electrons from ^{3}He in P. L. Anthony *et al.*, Phys. Rev. D **54**, 6620 (1996).
[15] The contribution of the neutron to the ^{129}Xe spin is estimated using the deviation of the observed magnetic moment from the expected shell model value in V. A. Dzuba, V. V. Flambaum, and P. G. Silvestrov, Phys. Lett. B **154**, 93 (1985).
[16] S. J. Asztalos *et al.*, Annu. Rev. Nucl. Part. Sci. **56**, 293 (2006).
[17] G. G. Raffelt, J. Phys. A **40**, 6607 (2007).
[18] A. N. Youdin *et al.*, Phys. Rev. Lett. **77**, 2170 (1996).
[19] C. L. Bennett *et al.*, Astrophys. J. Suppl. Ser. **148**, 1 (2003).
[20] I. K. Kominis *et al.*, Nature (London) **422**, 596 (2003).